FUBP1 Promotes Colorectal Cancer Stemness and Metastasis via DVL1-Mediated Activation of Wnt/β-Catenin Signaling

Haofan Yin
Sun Yat-sen University of Medical Sciences: Sun Yat-sen University Zhongshan School of Medicine
Tianxiao Gao
SYSU: Sun Yat-Sen University
Jinye Xie
SYSU: Sun Yat-Sen University
Zhijian Huang
SYSU: Sun Yat-Sen University
Xiaoyan Zhang
SYSU: Sun Yat-Sen University
Fengyu Yang
SYSU: Sun Yat-Sen University
Weiwei Qi
SYSU: Sun Yat-Sen University
Zhonghan Yang
SYSU: Sun Yat-Sen University
Ti Zhou
SYSU: Sun Yat-Sen University
Guoquan Gao
SYSU: Sun Yat-Sen University
Xia Yang (yangxia@mail.sysu.edu.cn)
Sun Yat-sen University Zhongshan School of Medicine

Research

Keywords: Colorectal cancer, Cancer stem cells, FUBP1

Posted Date: January 25th, 2021

DOI: https://doi.org/10.21203/rs.3.rs-152458/v1

Version of Record: A version of this preprint was published at Molecular Oncology on July 29th, 2021.
See the published version at https://doi.org/10.1002/1878-0261.13064.

Abstract

Background: Most colorectal cancer (CRC) patients die from distant metastasis. Approximately 50% of CRC patients develop liver metastases, while 10% to 30% of patients appear pulmonary metastases. The occurrence of metastasis is considered to be almost exclusively driven by cancer stem cells (CSCs) formation. However, the key molecules that confer the stem-transformation of CRC and subsequent metastasis remain unclear.

Methods: FUBP1 was screened in CRC CSCs by mass spectrometry and was examined by immunohistochemistry in a cohort of CRC tissues. The stemness induction and mechanism of FUBP1 were elucidated both *in vivo* and *in vitro*.

Results: FUBP1 was upregulated in 85% of *KRAS* mutation and 25% of wildtype CRC patients which correspondence to the metastasis rate. Further, elevated FUBP1 was positively correlated with CRC lymph node metastasis and clinical stages and negatively associated with overall survival, whatever *KRAS* mutation or wildtype. Overexpression of FUBP1 significantly enhanced migration, invasion, tumor sphere formation and CD133/ALDH1 expression of CRC cells *in vitro* and the tumorigenicity *in vivo*. Mechanistically, FUBP1 promoted the initiation of CSCs by activating Wnt/β-catenin signaling via directly binding to the promoter of DVL1, a vigoroso activator of β-catenin. The knockdown of DVL1 tremendously blockaded the stem-transformation and tumorigenicity of CRC. Activation of Wnt/β-catenin signaling by DVL1 increased pluripotent transcription factors, including c-Myc, NANOG, SOX2 rather c-Myc alone. Moreover, FUBP1 was upregulated at the post-transcriptional level. Elevated FUBP1 in *KRAS* wildtype CRC patients is due to the decrease of Smurf2, which promotes ubiquitin-mediated degradation of FUBP1. Whereas FUBP1 was upregulated in mutated *KRAS* patients through both inhibition of caspase-3-dependent cleavage and decreased Smurf2.

Conclusions: Our results demonstrate for the first time that FUBP1 is a novel oncogene for the initiation of CSCs as a new endogenous Wnt signaling powerful agonist and may provide an important prognostic factor and therapeutic target for metastasis in both *KRAS* mutation and wildtype CRC.

Background

Colorectal cancer (CRC) is the third leading cause of cancer death worldwide, and there is an increasing incidence of tumor metastasis before diagnosed, especially among young patients[1]. Most CRC patients die from recurrence and distant metastasis. Approximately 50% of patients with CRC develop liver metastases, while 10–30% of patients appear pulmonary metastases[2]. Metastasis is the main reason for the poor treatment and prognosis in CRC. Therefore, it is very urgent to elucidate the mechanism that leads to the metastasis of colorectal cancer and to find new molecular targets.

The occurrence of metastasis is considered to be almost exclusively driven by cancer stem cells (CSCs), which seeds and colonizes to distant organs[3, 4]. CSCs are a small subpopulation of cells that have been

defined by their tumor-initiating properties in colon, breast, head, lung and liver carcinomas[5]. It was found that $CD133^+$ CRC cells were more likely to metastasize than $CD133^-$ CRC cells in mice[6]. Additionally, the previous study showed that stem cell-related markers CD133, CD44, and ALDH1 were more highly expressed in tissues with lymph node metastasis tissues than in CRC primary cancer [7]. Furthermore, a recent study found that in CSC profiles have a high prognostic impact for CRC patients, which further supports the hypothesis that CRC strongly links to the presence of an altered stem cell subpopulation[5, 8]. Therefore, CSCs-targeted therapies might be an effective strategy to prevent metastasis of CRC. However, the key molecules that regulate colorectal cancer stem cells and subsequent metastasis remain unclear.

Far upstream element-binding protein 1 (FUBP1), a single-stranded DNA-binding protein, is highly expressed in various tumor cell lines and tissues, including liver cancer, renal cell carcinoma, squamous cell carcinoma, gastric cancer, breast cancer, non-small lung cancer and Hodgkin's lymphoma[9]. FUBP1 forms a complex with the far upstream element (FUSE) site to regulate gene expressions, including c-Myc, Usp29, p21, etc., which displays a broad spectrum of activities, such as promoting proliferation, inhibiting apoptosis of tumor cells[10, 11]. Our recent study revealed that elevated FUBP1 accelerated glycolysis resulting in neuroblastoma cell proliferation through inhibiting the degradation of HIF1α via binding to the VHL promoter[12]. Uta *et al.* showed that FUBP1 could inhibit the mRNA transcription of cell cycle suppressor p21 on maintaining the self-renewal of hematopoietic stem cells[13]. Hwang *et al.* found that FUBP1 regulated the selective splicing of LSD1 to change the maintenance of neural progenitor cells[14]. Josephine *et al.* revealed that knock-out of FUBP1 delayed the differentiation of embryonic stem cells to mesoderm[15]. These studies imply that FUBP1 is closely related to the maintenance and differentiation of stem cells. However, the expression and the exact role of FUBP1 in CRC and CRC-related CSCs have not been investigated.

In the present study, we aimed to identify the effects of FUBP1 on promoting colorectal cancer stemness and metastasis and the underlying mechanism.

Materials And Methods

Human samples

54 cases of CRC tissue samples were collected from Sun Yat-sen University Cancer Center. All patients' informed consent has been obtained before surgery, and the use of medical records and histological sections has also been approved by the ethics committee in SYUCC. The CRC tissue microarrays (HCol-Ade180Sur-08-M-088, 89 cases; HCol-A150CS-02-M-013, 75 cases) were purchased from Shanghai Outdo Biotech (Shanghai, China). All procedures were performed under consensus agreements and in accordance with the Chinese Ethical Review Committee. The clinical and biological characteristics of the patients were described in Supplementary Table 6.

Cell lines and culture

The human CRC cell lines (CaCO2, HCT-116, SW48, LoVo, SW620) were obtained from the American Type Culture Collection (Manassas, USA). The normal intestinal epithelial cell lines (NCM460, CCD841) were provided by Professor Peng Huang, from Sun Yat-sen University Cancer Center. Cell lines were authenticated by Cellcook Biotech Co., Ltd, (Guangzhou, China). KRASG13D SW48 was established by an improved CRISPR/Cas9-mediated precise genetic modification by using 1μM non-homologous end joining (NHEJ) inhibitor Scr7 (Selleck, S7742).

Western Blotting

Western blotting was performed according to a standard protocol, as described previously. The total proteins were collected using SDS lysis buffer (Beyotime, P0013G), and protein concentrations were determined by Bicinchoninic Acid (KeyGen, KGP902). Nuclear extracts were obtained using the NE-PER Nuclear and cytoplasmic extraction reagents (Thermo Scientific, Massachusetts, USA, 78833) according to the manufacturer's instructions. The following primary antibodies were used: FUBP1(ABE1330) from Merck Millipore (Boston, USA); CD133 (#86781), ALDH1 (#54135), CD44 (#37259), p-GSK3β (Ser9) (#9323), GSK3β (#9832), n-p-β-catenin (Ser33/37/Thr41)(#8814), β-catenin (#9582), Histone (4499) ,c-Myc (#13987) from Cell Signaling Technology (Boston, USA); LGR5 (ab75732), DVL1 (ab233003) from Abcam(Cambridge, UK); β-actin (A5441) from Sigma-Aldrich (St. Louis, USA). HRP-conjugated anti-rabbit IgG (Cell Signaling Tech, #7074) and anti-mouse IgG (Sigma-Aldrich, AP308P) were used as secondary antibodies. Proteins were determined using ECL Plus Reagent (Millipore, WBKLS0100).

RNA isolation and RT-qPCR

Gene expression validation by RT–qPCR was performed as previously described. The PCR primer sequences are listed in Supplementary Table 3.

Immunohistochemistry staining

Immunohistochemistry was performed according to a standard protocol as described previously. The slides were incubated with anti-FUBP1, anti-CD133, anti-ALDH1, or anti DVL1 monoclonal antibodies at 4°C overnight. On the second day, the slides were treated with HRP-conjugated secondary antibody and the antigen-antibody complex was visualized by incubation with the DAB kit. Finally, all sections were counterstained with hematoxylin and photographed through a slide scanner (Axio Scan. Z1, ZEISS, Oberkochen, Germany). The degree of immunostaining was determined by the staining index (SI). The SI was calculated as the product of the grade of tumor cell proportions and the staining intensity score. The tumor cell proportions were graded as follows: 0, no positive tumor cells; 1, < 10% positive tumor cells; 2, 10-35% positive tumor cells; 3, 35-75% positive tumor cells; and 4, > 75% positive tumor cells. Staining

intensity was scored as follows: 1, no staining; 2, weak staining (light yellow); 3, moderate staining (yellow-brown); and 4, strong staining (brown). Accordingly, the protein expression as evaluated by SI has a possible score of 0, 1, 2, 3, 4, 6, 8, 9, 12, or 16. Samples with SI ≥ 6 were determined as high expression, and those with SI < 6 were determined as low expression.

Immunofluorescence staining

After fixed in 4% paraformaldehyde, cells were blocked with goat serum at 37℃ for 1h. They were incubated with rabbit β-catenin antibody at 4°C overnight, then were incubated with FITC conjugated goat anti-rabbit IgG (Dako, Glostrup, Denmark, K500711) at 37℃ for 1 h after three times washing. Finally, the cell nucleus was stained with DAPI (Sigma-Aldrich, D9542). Cells were visualized under Olympus BX51. Five randomly picked fields per slide were analyzed to determine the nuclear β-catenin MOD, which represents the strength of staining signals as measured per positive pixels. MOD values for different groups of tissues were compared using the Student's t-test.

Migration and invasion assay

A total of 5×10^4 cells in 200 μl serum-free RPIM 1640 were seeded on cell culture inserts with 8 μm microporous filters (Corning, New York, USA, 26616) coated with (invasion) or without (migration) Matrigel (BD Biosciences, Franklin Lakes, USA), and 500 μl of RPIM 1640 containing 10% FBS was added to the lower chamber. After being incubated for 48h, the cells in the upper filters (inside the inserts) were removed, and the migrated or invaded cells in the lower filters (outside the inserts) were fixed in ethanol for 20 min, then stained with crystal violet for 10 min and counted under a microscope. The number of migrated or invaded cells in 5 random optical fields (×100 magnification) of each filter from triplicate inserts was averaged.

Tumor sphere formation assay

$1x10^3$ cells were seeded in 96-well ultra-low cluster plates (Corning, 3469) for 10 days. The tumor spheres were cultured in DMEM/F12 (Corning, R10-092-CV) serum-free medium supplemented with 2% B27 (Thermo Scientific, Cat. No. 12587010), 20 ng/mL epidermal growth factor (EGF, Beyotime, P5552), 20 ng/mL basic fibroblast growth factor (bFGF, Beyotime, P6443), 5 μg/mL insulin (Beyotime, P3376), and 0.4% BSA (Sigma-Aldrich, Cat. No. A1933-1G). After 10 days, the tumor spheres (tight, spherical, non-adherent masses > 50 μm in diameter) were counted, and their images were captured under an inverted microscope.

Luciferase reporter assay

Luciferase assay was performed using the Dual Luciferase Reporter Assay Kit (Promega, Madison, WI, USA) according to a protocol provided by the manufacturer.

Cell sorting and flow cytometry

BD Influx Cell Sorter was used to sort out cells. To obtain the $CD133^+ALDH1^+$ cells, LoVo cells were labeled with primary anti-CD133 (Thermo Scientific, 12-1331-82) monoclonal antibody. Aldefluor kit (STEMCELL Technologies, Vancouver, Canada) was used to analyze the population of cells with high ALDH enzymatic activity. Before isolation, samples were subsequently washed and resuspended into single-cell suspensions in phosphate buffered saline (PBS) for performing the separation. For the proportion of $CD133^+ALDH1^+$ cells detection, CRC cells were assessed and analyzed by flow cytometry using a CytoFLEX Flow Cytometer (Beckman Coulter, Pasadena, USA).

Chromatin immunoprecipitation (CHIP) assay

2×10^6 Cells plated in a 100 mm culture dish were treated with 1% formaldehyde to cross-link proteins to DNA. The cell lysates were sonicated to shear the DNA into 100–1000 bp lengths. Aliquots containing equal amounts of chromatin supernatants were incubated on a rocking bed at 4°C overnight with either 1 μg FUBP1 antibody, or 1 μg IgG antibody as a negative control. Following reverse cross-linking of protein–DNA complexes to free the DNA, PCR was carried out. The primers used in this study are listed in the online supplementary materials and methods.

Plasmids, retroviral infection, and transfection

All lentiviral vectors contained the puromycin resistance gene. Vectors encoding FUBP1 shRNAs were purchased from Hanbio Biotechnology Co., Ltd, (Shanghai, China). Vectors encoding DVL1 and c-Myc were purchased from GeneChem Co., Ltd, (Shanghai, China). FUBP1 siRNA, DVL1 siRNA, c-Myc siRNA and, control siRNA were purchased from RiboBio (Guangzhou, China). Plasmids encoding FUBP1 were purchased from Obio Technology Co., Ltd, (Shanghai, China); the lentiviruses were packaged, and cells were transduced and subjected to puromycin selection as previously described35. According to the manufacturer's instructions, transfections were performed at approximately 60% confluency using Lipofectamine 3000. After 48 hours, confirmation of interference or overexpression was carried out using Real-time quantitative PCR (RT-qPCR) and Western blotting. For sgRNA cloning, the CRISPR/Cas9 vector PX459 (Addgene, #62988) was digested with BbsI (Thermo Scientific, FD1014) and ligated with BbsI compatible annealed oligos. The sgRNA targeting the upstream sequence of KRAS exon2 (5'-GCATTTTTCTTAAGCGTCGATGG-3') was designed using Optimized CRISPR Design. The homologous fragments using for introducing the point mutation were amplified by overlapping PCR and assembled into T vector pGM-T (TianGen, VT202) using In-Fusion technology (Clontech, #639636). Next, the donor

vector using for homology-directed repair (HDR) was generated with the homologous fragment (amplified by overlapping PCR with attB1 at the ends) and pDONR (Thermo Scientific, #12536017) by BP reaction.

iTRAQ protein mass spectrometry

iTRAQ protein mass spectrometry was performed by PTM BIO Co., Ltd, (Hangzhou, China) according to a standard protocol. The MaxQuant (version 1.4.1.2) software was used to analyze the raw data by GeneChem Co., Ltd, (Shanghai, China).

Tumor xenograft

Male BALB/c nude mice (4-weeks-old, 16-18 g) were purchased from Beijing Vital River Laboratory Animal Technology Co., Ltd. (Beijing, China). Based on a previously described standard protocol, the mice were randomly divided into the indicated groups. SW48 or LoVo cells (1×10^6, 1×10^5, 1×10^4, or 1×10^3), stably transfected with FUBP1-silenced, FUBP1 or vector, were inoculated into the inguinal folds of mice (n = 6 in each cell line per group). Also, CD133+ALDH1+ CSCs (1×10^5, 1×10^4, 1×10^3, or 1×10^2) sorted from LoVo cells, stably transfected with FUBP1-silenced or vector, were inoculated into the inguinal folds of mice. Tumor volumes were measured with an external caliper and calculated using the equation $(L \times W^2)/2$. At 28 days after inoculation, the mice were sacrificed, and the tumors were excised and subjected to pathologic examination. All procedures are related to animal feeding, treatment and welfare were conducted in accordance with the Institutional Animal Care and Use Committee of Sun Yat-sen University.

Statistical analysis

The variability of the data is presented as the SD (mean±SD) and was assessed with Student's t-test between two groups. For multiple groups, significant differences were determined using one-way ANOVA. The relationships between FUBP1 expression and clinicopathological characteristics were determined using the $\chi 2$ test. Survival curves were plotted using the Kaplan-Meier method and compared using the log-rank test. Survival data were evaluated using univariate and multivariate Cox regression analyses. Tumorigenic cell frequency (TIC) was calculated based on extreme limiting dilution analysis (ELDA) (http://bioinf.wehi.edu.au/software/elda/). Statistical significance was defined at $p<0.05$.

Results

Elevated FUBP1 is associated with tumor progression in CRC

LoVo cells derived from metastatic tumor tissue exhibited the strong ability of tumor sphere formation compared to SW48 cells derived from the primary site with low expression of CD133/ALDH

(Supplementary Figure. 1). To explore the critical functional molecules in tumor stemness and aggressiveness, we sorted $CD133^{+}ALDH1^{+}$ LoVo cells which accounted for a 9.6% ratio in total LoVo cells. We then analyzed differential protein expression between $CD133^{+}ALDH1^{+}$ LoVo cell and SW48 cells by iTRAQ protein mass spectrometry (Figure. 1A). Among the most changed proteins, a transcription factor, FUBP1, draws our attention. Since it is closely related to the maintenance and differentiation of stem cells, while the connection of FUBP1 with CRC was barely mentioned before (Figure. 1B-C).

Next, we verified the crucial role of FUBP1 in the progression of CRC. Impressively, compared to adjacent specimens (H-Score = 1.411), FUBP1 expression was remarkably increased in CRC specimens (H-Score = 4.089; $p < 0.001$; Figure. 1D-E) in a CRC Tissue Microarray (Supplementary Figure. 2). Meanwhile, we retrospectively studied the medical records of 143 patients in the CRC population and identified that FUBP1 expression increased along with the progression of CRC clinical stages (Figure. 1F-G). In addition, Correlation analysis demonstrated that elevated FUBP1 positively correlated with CRC lymph node metastasis and advanced clinical stages (Supplementary Table. 1). Accordingly, FUBP1 expression was negatively associated with overall survival ($p < 0.001$; Figure. 1H). The OS of the FUBP1 high expression group was even 30.25 months shorter than that of the low expression group (HR, 1.96; 95% CI, 1.291 to 2.974). Taken together, the upregulation of FUBP1 is associated with CRC metastasis and might be a potential prognostic factor for CRC.

Elevated Fubp1 Promotes Crc Cells Migration And Invasion

Similar to the results in CRC tissues, FUBP1 was significantly increased in CRC cell lines compared with normal intestinal epithelial cells (NCM460, CCD841). Moreover, CRC cells (LoVo, SW620) derived from tumor metastasis showed higher expression of FUBP1 than those (CaCO2, HCT116, SW48) derived from the primary site (Figure. 2A-B).

Furthermore, colony formation assay was performed to validate the cloning ability of CRC cells promoted by FUBP1. As shown in Figure. 2C-D, compared to the vector control cells, the numbers of the colony from FUBP1-transfected SW48 cells increased, and conversely decreased in FUBP1-silenced LoVo cells (Supplementary Figure. 3A-B). Moreover, Transwell and wound healing assay showed that the migration and invasion abilities were substantially enhanced in FUBP1 overexpressed SW48 cells, while were suppressed in FUBP1 knocked down LoVo cells (Figure. 2E-H; Supplementary Figure. 3C-F). These results suggested that the upregulation of FUBP1 promoted CRC cell migration and invasion.

Elevated FUBP1 promotes the stemness of CRC cells in vitro

CRC recurrence and distant metastasis arise from a subpopulation of CSCs, and FUBP1 expression was inversely correlated with tumor differentiation status (Supplementary Table. 1), which implied that cell migration and invasion enhanced by FUBP1 might be attributed to the regulation of stemness. To explore the oncogenic role of FUBP1 in the stimulation of stemness in CRC cells, firstly, the protein levels of the stemness-related markers, CD133, ALDH1, LGR5, and CD44, were examined between FUBP1 low

expressing SW48 cells and FUBP1 high expressing LoVo cells. It showed that expression of stemness-related markers, especially CD133 and ALDH1, were elevated in the LoVo cell (Supplementary Figure.1A). Meanwhile, western blotting results revealed that CD133 and ALDH1, were up-regulated in FUBP1-transfected SW48 cells, and conversely downregulated in FUBP1-silenced LoVo cells (Figure. 3A; Supplementary Figure. 4A). In addition, Flow cytometry results further showed that overexpression of FUBP1 substantially increased the $CD133^{+}ALDH1^{+}$ percentage in SW48 cells from 0.34–3.27%, while knockdown of FUBP1 decreased the $CD133^{+}ALDH1^{+}$ percentage in LoVo cells from 7.06–3.28% (Figure. 3B-C; Supplementary Figure. 4B-C).

Next, we conducted the tumor sphere formation assays to examine the effect of FUBP1 on the self-renewal ability of spherogenic CRC cells. After 10 days culture, the numbers and sizes of the formed spheres in the FUBP1-transfected SW48 group were more remarkable than that of the vector control group, and the FUBP1-silenced LoVo group exhibited the opposite effect (Figure. 3D-E; Supplementary Figure. 4D-E). Furthermore, FUBP1-transfected SW48 cells formed a more significant number of offspring spheres than the vector control cells, whereas FUBP1-silenced cells formed fewer offspring spheres (Figure. 3F).

To further confirm that FUBP1 played a considerable role in CRC CSCs, we investigated the expression of FUBP1 in $CD133^{+}ALDH1^{+}$ cells sorted from LoVo cells by flow cytometer. As expected, $CD133^{+}ALDH1^{+}$ LoVo cells expressed higher level of FUBP1 than the LoVo cells (Figure. 3G). Similarly, LoVo spheres sorted by tumor sphere formation also showed higher FUBP1 levels than the LoVo cells (Figure. 3H). while CD133 and ALDH1 were significantly down-regulated in FUBP1-silenced LoVo spheres (Figure. 3I). Notably, knockdown of FUBP1 in LoVo spheres substantially reduced the numbers and sizes of the formed spheres, and decreased the migration and invasion abilities (Figure. 3J-K; Supplementary Figure. 6). Collectively, these results indicated that the upregulation of FUBP1 promoted the stemness of CRC cells *in vitro*.

Elevated FUBP1 enhances the stemness and tumorigenicity of CRC cells in vivo

To explore the oncogenic role of FUBP1 in the promotion of stemness in CRC cells *in vivo*, BALB/c nude mice were subcutaneously inoculated different numbers of CRC cells mixed with Matrigel into the inguinal folds. The tumors formed by FUBP1-transfected SW48 cells had a larger size and obvious tumorigenicity than those formed by vector control cells after implantation of 1×10^{6}, 1×10^{5}, 1×10^{4}, or 1×10^{3} cells (Figure. 4A-B; Supplementary Table. 2). Conversely, FUBP1-silenced LoVo cells formed smaller tumors and had blunt tumorigenicity (Figure. 4C-D; Supplementary Table. 2). Notably, the tumorigenicity of the sorted $CD133^{+}ALDH1^{+}$ LoVo cells was enhanced and fewer implantation of 1×10^{5}, 1×10^{4}, 1×10^{3}, or 1×10^{2} cells were needed, meanwhile tumor size and tumorigenicity were quelled by FUBP1-silence (Figure. 4E-F; Supplementary Table. 3). Western blotting and Immunohistochemistry (IHC) results demonstrated that the expression of CD133 and ALDH1 in tumors originated from FUBP1-transfected SW48 cells were increased, compared with that from vector control cells (Figure. 4G; Supplementary Figure. 7). Notably, the expression of CD133 ($p < 0.001$; $R^2 = 0.519$) and ALDH1 ($p < 0.001$; $R^2 = 0.588$) in

human CRC specimens were strongly positively correlated with FUBP1 in a CRC Tissue Microarray (Figure. 4H-I; Supplementary Figure. 8). Therefore, we concluded that elevated FUBP1 enhanced the stemness and tumorigenicity of CRC cells *in vivo*.

Elevated FUBP1 mediates stemness through the activation of the Wnt/β-catenin signaling

Wnt/β-catenin signaling is well accepted to be involved in the stemness in CRC[8]. To explore the mechanism related to the FUBP1-mediated stemness in CRC, we observed the Wnt/β-catenin signaling in the indicated FUBP1-transfected, FUBP1-silenced, or vector control cells. As expected, FUBP1 positively regulated the phosphorylation level of GSK-3β (Ser9) and non-phosphorylation levels of β-catenin (Figure. 5A). Next, nuclear extract and immunofluorescence assays showed that overexpression of FUBP1 substantially increased the β-catenin nuclear signals, whereas knockdown of FUBP1 reduced β-catenin nuclear translocation (Figure. 5B-D). Meanwhile, the mRNA transcription of the downstream targets of Wnt/β-catenin signaling, including COX2, MMP7, CCND1, c-MYC, and SOX2, were increased in FUBP1-transfected cells but were decreased in FUBP1-silenced cells (Figure. 5E). Collectively, these data suggested that FUBP1 overexpression activated the Wnt/β-catenin signaling pathway.

To further validated the targets of FUBP1 in the Wnt/β-catenin signaling pathway, we used Real-time PCR to detect the change of receptors and ligands which played essential roles in this pathway, including LRP5, LRP6, FZD1, WNT3A, and WNT5A, as FUBP1 had been proved to be an important transcription factor. However, none of these molecules are significantly altered (Supplementary Figure. 9). Then, we detected mRNA levels of the critical scaffold molecules in the upstream of β-catenin, including DVL, GSK-3β, APC, AXIN, and CK1. Impressively, we found that DVL1 mRNA levels were significantly up-regulated by FUBP1, while other molecules remained unchanged (Figure. 5F). Moreover, FUBP1 increased DVL1 protein expression levels in CRC cells and tumor specimens, whereas silencing FUBP1 had the opposite effects (Figure. 5G; Supplementary Figure. 7). Furthermore, FUBP1 expression was positively correlated with the expression of DVL1 in CRC tissues ($p < 0.001$; $R^2 = 0.541$; Figure. 5H-I). These data indicated that FUBP1 activates the Wnt/β-catenin signaling through transcriptionally regulating DVL1.

Fubp1 Up-regulates Dvl1 Through Direct Binding To Its Promoter

To investigate how DVL1 was transcriptionally regulated by FUBP1, promoter assays were undertaken. As shown in Figure. 6A, luciferase reporters containing the full-length of the human DVL1 promoter were transiently transfected into LoVo cells and overexpressed FUBP1 vector or empty vector as a control. Overexpression of FUBP1 significantly increased DVL1 promoter-driven reporter activity. To identify the specific binding site, we constructed five truncation fragments of DVL1 promoter, as indicated in Supplementary Figure. 11A. Our results demonstrated that FUBP1 is bound to DVL1-P3 fragments (Figure. 6B). After carefully searching, we found a potential binding site (TTCCCCTGATTT) in DVL1-P3 fragments was identical to the c-Myc FUSE binding site. The candidate FUBP1 binding site,

TTCCCCTGATTT, was shown in the − 1178 to − 1167 region of the DVL1 promoter sequence (Figure. 6C). To confirm whether FUBP1 can directly bind to this site, we constructed a mutation of DVL1-P3 (C to G substitution and T to A substitution, underlined), and the mutation abolished FUBP1 mediated up-regulation of DVL1-P3 promoter reporter activity. Chromatin immunoprecipitation (ChIP) assays further confirmed that FUBP1 could directly bind to DVL1-P3 fragments (Figure. 6D; Supplementary Figure. 10A).

Next, we investigated whether DVL1 activation was required for the stemness in CRC cells. Silencing DVL1 substantially reduced the sphere-forming ability of FUBP1-overexpressing cells, the stemness-related markers expressions (CD133 and ALDH1), as well as Wnt/β-catenin signaling (Figure. 6E-F; Supplementary Figure. 10B). The increased abilities of CRC cell migration and invasion induced by overexpression of FUBP1 were also dramatically abrogated by knockdown of DVL1 (Supplementary Figure. 11B-C). Moreover, to address the key role of DVL1 in the FUBP1-induced effect of CRC *in vivo*, we generated a cell line-derived xenograft model using SW48-Vector, SW48-FUBP1, SW48-FUBP1 with DVL1 knockdown, and SW48-FUBP1 with NSC668036 treatment (DVL inhibitor). It showed that SW48-FUBP1 with DVL1 knockdown and treatment with NSC668036 in SW48-FUBP1 xenografts inhibited the tumor volume and tumorigenicity significantly(Figure. 6G-H; Supplementary Table. 4). On the contrary, LoVo-FUBP1 with DVL1 overexpression xenografts recovered the tumor volume and tumorigenicity compared with LoVo-shFUBP1 xenografts (Figure. 6I-J; Supplementary Table. 5). Taken together, our results indicated that FUBP1 activated the Wnt/β-catenin signaling to promote the stemness of CRC cells through up-regulating DVL1 by direct binding to DVL1's promoter.

FUBP1 is ubiquitinated by Smurf2 in CRC regardless of KRAS genotype

The above data suggest that FUBP1 plays a crucial role in the stemness and metastasis in CRC. The critical question arose up that the intrinsic mechanism by which FUBP1 was up-regulated in CRC. *KRAS* mutations are the most frequent alterations, occurring in 30–50% of CRC cases. Further investigation of 54 CRC specimens identified that FUBP1 was highly expressed in *KRAS* mutation CRC specimens (n = 14) compared with *KRAS* wild-type specimens (n = 40; $p < 0.001$; Figure. 7A-B). The proportion of high FUBP1 expression (H-Score ≥ 6) in the *KRAS* mutation group (85.71%, 12/14) was higher than that of the *KRAS* wild-type group (25.00%,10/40; Figure. 7C). Moreover, *KRAS* mutation significantly increased FUBP1 protein expression levels in CRC cells, whereas silencing *KRAS* exhibited the opposite effects (Supplementary Figure. 12C). Unexpectedly, the RNA level of FUBP1 was unchanged in the tumor section than adjacent sections from the TCGA-COAD database, and remain consistent in the LoVo cell compared to the SW48 cell (Supplementary Figure. 12A-B).

Interestingly, we found that the proportion of high FUBP1/*KRAS* wild-type specimen remained as 18.52% of total CRC pathological samples (10/54; Figure. 7C). The survival outcomes of patients with high FUBP1 expression in both *KRAS* wild-type (HR, 2.369; 95%CI, 0.923 to 6.080; $p = 0.013$) and *KRAS* mutation (HR, 5.201; 95%CI, 1.612 to 16.78; $p < 0.001$) were much poorer compared with simultaneous low FUBP1 /*KRAS* wild-type patients (Figure. 7D). While the survival outcomes of patients had no statistical difference between high FUBP1/*KRAS* wild-type and high FUBP1/*KRAS* mutation groups ($p =$

0.066; Figure. 7D). While FUBP1 RNA levels were not statistically different in CRC specimens between *KRAS* mutation, *KRAS* wild-type, and adjacent CRC specimens (Supplementary Figure. 12D). These results suggest that FUBP1 might be post-transcriptionally regulated in CRC regardless of *KRAS* mutation.

Recently studies showed that Smurf2 was responsible for the ubiquitination of FUBP1. Excitingly, lower expression of Smurf2 was found only in the high FUBP1/ *KRAS* wild-type group (Figure. 7E-F). Silencing Smurf2 substantially increased the expression of FUBP1 and the stemness-related markers, CD133 and ALDH1, conversely decreased in Smurf2 overexpressed cells (Figure. 7G). Consistently, we found Smurf2 effectively shorten protein half-lives of FUBP1 via proteasomal degradation pathway (Figure. 7H-I). Furthermore, ectopically expressed Smurf2 with MG132 treatment markedly promoted the polyubiquitination levels of FUBP1 (Figure. 7J). These data indicated that the FUBP1 level was post-transcriptionally by Smurf2 in *KRAS* mutation and part of *KRAS* wild-type CRC.

FUBP1 is also up-regulated by caspase3 inactivation driven by KRAS **signaling in** KRAS **mutation CRC**

Moreover, Previous research demonstrated that FUBP1 was the hydrolyzed substrate of caspase3[11], which is mainly suppressed by the anti-apoptosis AKT and ERK signaling. *KRAS* mutation, which directly activates ERK and AKT pathways, has been recently linked to CSCs-like phenotypes[16]. Therefore, we hypothesized that inhibition of caspase3 activity through activating the anti-apoptosis AKT and ERK signaling mediated by *KRAS* mutation also contributed to the abnormal increase of FUBP1.

Next, we observed the protein expression induction of FUBP1 in SW48 treated with SC79 (AKT activator), LM22B-10 (ERK activator), Nocodazole (apoptosis activator) or *KRAS* mutation, along with FUBP1 expression in LoVo treated with MK2206 (AKT inhibitor), AZD0364 (ERK inhibitor), Z-VAD-FMK (apoptosis inhibitor) or KRAS knockdown (Figure. 8A). It showed that AKT and ERK activators increased the expression of FUBP1 in SW48 almost close to that of SW48 $KRAS^{G13D}$, while apoptosis agonist could block this induction. On the contrary, AKT and ERK inhibitors decreased the expression of FUBP1 in LoVo almost close to that of LoVo-shKRAS, while apoptosis inhibitor rescued this inhibition. Silencing FUBP1 substantially reduced the stemness inducing by *KRAS* mutation (Figure. 8B-D). All these data confirmed that FUBP1 was post-transcriptionally up-regulated by caspase3 inhibition through AKT and ERK activation driven by *KRAS* mutation. The conclusion of the mechanism study fully revealed the reason for the increase of FUBP1 in colorectal cancer, providing another target for treatment (Figure. 8E).

Discussion

In this study, we revealed that FUBP1 is associated with tumor progression and metastasis in CRC tissues and cell lines (Figure. 1–2). Overexpression or knockdown of FUBP1 in CRC cells substantially enhanced or reduced the expression levels of CD133 and ALDH1, the formation of tumor sphere, thus affecting the ability of cell migration and invasion (Figure. 2–3). Consistently, *in vivo* results demonstrated that overexpression of FUBP1 significantly enhanced the tumorigenicity of CRC cells (Figure. 4). Mechanistically, FUBP1 promoted the initiation of CSCs by activating Wnt/β-catenin signaling via directly

binding to the promoter of DVL1. Further, KRAS up-regulated FUBP1 through inhibition of caspase-3-dependent cleavage, as well as the decrease of Smurf2, which promotes ubiquitin-mediated degradation accounted for the increase of FUBP1 in both *KRAS* wild-type and mutated CRC patients. Our investigation put forward the possibility of a novel therapeutic strategy for CRC stemness by inhibtion of FUBP1-centred pathway in mCRC patients.

FUBP1 could directly bind to the promoter of c-Myc[11]. Several studies have suggested that c-Myc played a critical role in regulating stem cell self-renewal[17], and was reported to promote the CSCs-like population of CRC cells[18]. Therefore, we need to evaluate the role of c-Myc in FUBP1-mediated stemness of CRC. As expected, overexpression of FUBP1 significantly increased c-Myc expression in CRC cells, whereas silencing FUBP1 had the opposite effects (Supplementary Figure. 13A). However, Silencing c-Myc could not completely reduce the sphere-forming ability of FUBP1-overexpressing cells and the expression of stemness-related markers, CD133, and ALDH1 in FUBP1-overexpressing CRC cells. Overexpression of c-Myc failed to wholly rescue the sphere-forming ability of FUBP1-silencing cells and the expression of stemness-related markers (Supplementary Figure. 13B-C). Whereas, the increased formation of tumor sphere, the abilities of CRC cell migration and invasion, the expression of stemness-related markers, and Wnt/β-catenin signaling induced by FUBP1 overexpression were dramatically eliminated by knockdown of DVL1(Figure. 6F-H; Supplementary Figure. 8B-C). In vivo expreiments futher showed DVL1 was crucial to the tumor volume and tumorigenicity in CDX animal model (Figure. 6G-J). Taken together, elevated FUBP1 promoted the stemness of CRC cells largely dependent on DVL1 rather than single c-Myc (Supplementary Figure. 12).

DVL has been considered as a crucial inter-mediates of Wnt/β-catenin signaling pathways, which inhibits GSK-3β, AXIN, and APC complex formation, regulating the generation of cell polarity, embryonic induction, and specification of cell fate[19]. DVL1 was also reported to be associated with distant metastasis and overall survival in breast cancer patients[20]. Meanwhile, DVL1 was noticeably up-regulated in CRC patients with liver metastasis, conferring a poor prognosis[21]. Notably, overexpression of DVL1 in HCC was observed to activate Wnt/β-catenin signaling pathway, thereby enhancing tumorigenicity and promoting a CSCs-like phenotype[22]. However, the relationship between FUBP1 and DVL1 had never been reported. Luciferase and chip assays confirmed that FUBP1 activated the Wnt/β-catenin signaling by directly binding to the DVL1 promoter in CRC cells (Figure. 6A-D). Moreover, the activation of Wnt/β-catenin signaling was responsible for the upregulation of pluripotent transcription factors c-MYC[17], SOX2[23], and NANOG[24] (Supplementary Figure. 5) and stemness induction of CRC cells (Figure. 6E-F). These results indicated for the first time that elevated FUBP1 promoted the stemness of mCRC by activating Wnt/β-catenin signaling.

Collectively, we first identified that FUBP1 acts as a transcriptional factor for DVL1, and the induction of CRC stemness mainly depends on the activation of the DVL1/Wnt/β-catenin pathway induced by FUBP1. The highlights of our study are to identify a new target gene of FUBP1 as a transcription factor, in other words, to append a new Wnt signaling agonist. This finding provides a novel strategy for the treatment of

metastatic CRC by targeting FUBP1 and DVL1. One limitation in the present study is that though one paper designed and generated FUBP1 small molecular inhibitor[25], it is not available for us to test whether this inhibitor can be therapeutically employed in CRC treatment. Since FUBP1 is a transcriptional factor and DVL is the main functional molecule in cytoplasm, we speculate that DVL1 may be more effective and less side effects as a therapeutic target. A specific small-molecule inhibitor binding to the DVL1 PDZ domain has just been identified and used as a treatment for fibrotic lung disease[26, 27]. It is worth investigating the effect of this specific small-molecule inhibitor in mCRC patients in the following work. Moreover, FUBP1 expression increased in several types of cancers[9], further exploring the role of FUBP1 and DVL1 on stemness transformation and metastasis in those cancers will broaden its significance.

A string of gene mutations characterizes the development of CRC. Among which, *KRAS* mutations are the most frequent alterations, occurring in 30–50% of CRC cases[28]. *KRAS* mutation has been recently linked to CSCs-like phenotypes, with functional characteristics of promoting tumor initiation, self-renewal, and metastasis in CRC cells [16]. Clinical evidence has revealed the association of the poor prognosis and liver metastasis with CSCs of *KRAS* mutation CRC patients[29]. Furthermore, metastasis also occurs in a small proportion of *KRAS* wild-type patients, which surprisingly has similar CSCs-like phenotypes in the corresponding cells[30]. Remarkably, the elevated FUBP1 was also observed in about 20% of *KRAS* wild-type CRC patients with poorer survival outcomes (Figure. 7C-D). These data indicated that FUBP1 possesses the same critical role in KRAS wild-type CRC, and its regulation was independent of KRAS mutation.Thus, uncovering the unique mechanism is necessary.

The elevated FUBP1 only occurred in the protein level rather than the mRNA level in mCRC, and then the post-transcriptionally regulation was mainly focused. Smurf2 is a member of the homologous to E6-AP carboxyl terminus family of E3 ubiquitin ligases that is important for the ubiquitination of several substrates, including SMAD2, SMAD7 and YY1[31]. Recent studies reported that Smurf2 was responsible for the ubiquitination of FUBP1, while low expression of Smurf2 was significantly associated with impaired overall survival of CRC patients[32, 33]. Our data showed that the expression of FUBP1 was negatively related to Smurf2 in *KRAS* wild-type patients. Silencing Smurf2 substantially increased the expression of FUBP1 and the stemness-related markers (Figure. 8G-I). These results confirmed that FUBP1 was regulated by Smurf2 in CRC. The finding provided insight for the additional treatment of mCRC with poor prognosis by up-regulating Smurf2. Smurf2 expression should be recommended to predict the therapeutic response in mCRC.

As *KRAS* mutation mediates aberrant ERK and AKT signaling transduction, agents targeted these two pathways were developed. However, targeted therapies by either AKT or ERK pathway inhibitors all failed in the second phase clinical trials[34, 35, 36]. The reason is mainly ascribed to the feedback activation of PI3K/AKT signaling after inhibiting RAS/RAF/MEK/ERK transduction or the drug toxicity of combining ERK and AKT inhibitors[37, 38, 39]. The long-term efforts to target the cancer-associated *KRAS* mutant were unsuccessful. In this study, we for the first time reported that FUBP1 functions as a stemness stimulator

in CRC. Selectively targeting FUBP1/DVL1, a novel downstream of *KRAS* signaling may be an alternative therapeutic strategy with less toxicity and side effects for *KRAS* mutation CRC.

Conclusion

In summary, our research demonstrates that elevated FUBP1 in CRC directly up-regulates DVL1 and activates the Wnt/β-catenin pathway, thereby enhancing stemness, promoting metastasis, and conferring a poor prognosis. This study also indicates that FUBP1 is a novel and powerful oncogene for the initiation of CSCs and may provide an important prognostic factor and therapeutic target for the efficient elimination of both *KRAS* mutation and wild-type CRC metastasis.

Abbreviations

CRC: Colorectal cancer; CSCs: cancer stem cells; FUBP1: Far upstream element-binding protein 1; IHC: Immunohistochemistry; CHIP: Chromatin immunoprecipitation; Real-time PCR: Quantitative real-time polymerase chain reaction

Declarations

Acknowledgements

The authors would like to acknowledge the helpful comments on this paper received from the reviewers.

Authors' Contributions

YX, GGQ, and ZT were responsible for designing and supervising the entire study and revised the manuscript. YHF, GTX, and XJY performed the experiments and analyzed the data. HZJ, ZXY, YFY, QWW, YZH contributed the data analysis and discussion.

Funding

This study was supported by the National Nature Science Foundation of China, grant numbers: 81872165, 81770808, 81572342, 81570871, and 81570764, and 81572409; National Key R&D Program of China (2018YFA0800400); Guangdong Provincial Key R&D Program (2018B030337001); the Key Project of Nature Science Foundation of Guangdong Province, China, grant numbers: 2016A030311035; the Guangdong Science Technology Project, grant numbers: 2020A1515010365, 2019A1515011810, 2017A020215075 and 2015B090903063; Initiate Research Funds for the Central Universities of China (Youth Program), grant numbers: 14ykpy05; the Key Sci-tech Research Project of Guangzhou Municipality, China, grant numbers: 201508020033, 201707010084, 201803010017, and 201807010069; the Pearl River Nova Program of Guangzhou Municipality, China, grant number: 201610010186; and the 2017 Milstein Medical Asian American Partnership Foundation Research Project Award in Translational Medicine; Science and Technology Program of Guangzhou, China (1563000305).

Availability of data and materials

All data generated or analysed during this study are included in this published article.

Ethics approval

All procedures are related to animal feeding, treatment and welfare were conducted in accordance with the Institutional Animal Care and Use Committee of Sun Yat-sen University.

Consent for publication

Not applicable.

Competing Interests

The authors declare no conflict of interest.

References

1. Siegel RL, Miller KD, Jemal A. Cancer statistics. 2018. *CA: a cancer journal for clinicians* 2018, **68**(1): 7–30.
2. Tan KK, Lopes Gde L Jr, Sim R. How uncommon are isolated lung metastases in colorectal cancer? A review from database of 754 patients over 4 years. Journal of gastrointestinal surgery: official journal of the Society for Surgery of the Alimentary Tract. 2009;13(4):642–8.
3. Gao W, Chen L, Ma Z, Du Z, Zhao Z, Hu Z, et al. Isolation and phenotypic characterization of colorectal cancer stem cells with organ-specific metastatic potential. Gastroenterology. 2013;145(3):636–46 e635.
4. Dieter SM, Ball CR, Hoffmann CM, Nowrouzi A, Herbst F, Zavidij O, et al. Distinct types of tumor-initiating cells form human colon cancer tumors and metastases. Cell stem cell. 2011;9(4):357–65.
5. Saygin C, Matei D, Majeti R, Reizes O, Lathia JD. Targeting Cancer Stemness in the Clinic: From Hype to Hope. Cell stem cell. 2019;24(1):25–40.
6. Li G, Liu C, Yuan J, Xiao X, Tang N, Hao J, et al. CD133(+) single cell-derived progenies of colorectal cancer cell line SW480 with different invasive and metastatic potential. Clin Exp Metastasis. 2010;27(7):517–27.
7. Zeuner A, Todaro M, Stassi G, De Maria R. Colorectal cancer stem cells: from the crypt to the clinic. Cell stem cell. 2014;15(6):692–705.
8. Vermeulen L, De Sousa EMF, van der Heijden M, Cameron K, de Jong JH, Borovski T, et al. Wnt activity defines colon cancer stem cells and is regulated by the microenvironment. Nat Cell Biol. 2010;12(5):468–76.
9. Debaize L, Troadec MB. The master regulator FUBP1: its emerging role in normal cell function and malignant development. Cell Mol Life Sci. 2019;76(2):259–81.

10. Zhang J, Chen QM. Far upstream element binding protein 1: a commander of transcription, translation and beyond. Oncogene. 2013;32(24):2907–16.
11. Jang M, Park BC, Kang S, Chi SW, Cho S, Chung SJ, et al. Far upstream element-binding protein-1, a novel caspase substrate, acts as a cross-talker between apoptosis and the c-myc oncogene. Oncogene. 2009;28(12):1529–36.
12. Jiang P, Huang M, Qi W, Wang F, Yang T, Gao T, et al. FUBP1 promotes neuroblastoma proliferation via enhancing glycolysis-a new possible marker of malignancy for neuroblastoma. Journal of experimental clinical cancer research: CR. 2019;38(1):400.
13. Rabenhorst U, Thalheimer FB, Gerlach K, Kijonka M, Bohm S, Krause DS, et al. Single-Stranded DNA-Binding Transcriptional Regulator FUBP1 Is Essential for Fetal and Adult Hematopoietic Stem Cell Self-Renewal. Cell reports. 2015;11(12):1847–55.
14. Hwang I, Cao D, Na Y, Kim DY, Zhang T, Yao J, et al. Far Upstream Element-Binding Protein 1 Regulates LSD1 Alternative Splicing to Promote Terminal Differentiation of Neural Progenitors. Stem cell reports. 2018;10(4):1208–21.
15. Wesely J, Steiner M, Schnutgen F, Kaulich M, Rieger MA, Zornig M. Delayed Mesoderm and Erythroid Differentiation of Murine Embryonic Stem Cells in the Absence of the Transcriptional Regulator FUBP1. Stem cells international. 2017;2017:5762301.
16. Moon BS, Jeong WJ, Park J, Kim TI, Min do S, Choi KY. Role of oncogenic K-Ras in cancer stem cell activation by aberrant Wnt/beta-catenin signaling. J Natl Cancer Inst. 2014;106(2):djt373.
17. Fagnocchi L, Zippo A. Multiple Roles of MYC in Integrating Regulatory Networks of Pluripotent Stem Cells. Frontiers in cell developmental biology. 2017;5:7.
18. Elbadawy M, Usui T, Yamawaki H, Sasaki K. Emerging Roles of C-Myc in Cancer Stem Cell-Related Signaling and Resistance to Cancer Chemotherapy: A Potential Therapeutic Target Against Colorectal Cancer. *International journal of molecular sciences* 2019, 20(9).
19. Wallingford JB, Habas R. The developmental biology of Dishevelled: an enigmatic protein governing cell fate and cell polarity. Development. 2005;132(20):4421–36.
20. Zeng B, Li Y, Feng Y, Lu M, Yuan H, Yi Z, et al. Downregulated miR-1247-5p associates with poor prognosis and facilitates tumor cell growth via DVL1/Wnt/beta-catenin signaling in breast cancer. Biochem Biophys Res Commun. 2018;505(1):302–8.
21. Yang W, Chang Y, Huang H, Wang Y, Yu X. Association between Obesity, Serum Lipids, and Colorectal Polyps in Old Chinese People. Gastroenterol Res Pract. 2013;2013:931084.
22. Song J, Xie C, Jiang L, Wu G, Zhu J, Zhang S, et al. Transcription factor AP-4 promotes tumorigenic capability and activates the Wnt/beta-catenin pathway in hepatocellular carcinoma. Theranostics. 2018;8(13):3571–83.
23. Atkinson PJ, Dong Y, Gu S, Liu W, Najarro EH, Udagawa T, et al. Sox2 haploinsufficiency primes regeneration and Wnt responsiveness in the mouse cochlea. J Clin Investig. 2018;128(4):1641–56.
24. Pan G, Thomson JA. Nanog and transcriptional networks in embryonic stem cell pluripotency. Cell research. 2007;17(1):42–9.

25. Hauck S, Hiesinger K, Khageh Hosseini S, Achenbach J, Biondi RM, Proschak E, et al. Pyrazolo[1,5a]pyrimidines as a new class of FUSE binding protein 1 (FUBP1) inhibitors. Bioorg Med Chem. 2016;24(22):5717–29.
26. Wang C, Dai J, Sun Z, Shi C, Cao H, Chen X, et al. Targeted inhibition of disheveled PDZ domain via NSC668036 depresses fibrotic process. Experimental cell research. 2015;331(1):115–22.
27. Shan J, Shi DL, Wang J, Zheng J. Identification of a specific inhibitor of the dishevelled PDZ domain. Biochemistry. 2005;44(47):15495–503.
28. Vogelstein B, Fearon ER, Hamilton SR, Kern SE, Preisinger AC, Leppert M, et al. Genetic alterations during colorectal-tumor development. N Engl J Med. 1988;319(9):525–32.
29. Nash GM, Gimbel M, Shia J, Nathanson DR, Ndubuisi MI, Zeng ZS, et al. KRAS mutation correlates with accelerated metastatic progression in patients with colorectal liver metastases. Ann Surg Oncol. 2010;17(2):572–8.
30. Zhang P, Holowatyj AN, Roy T, Pronovost SM, Marchetti M, Liu H, et al. An SH3PX1-Dependent Endocytosis-Autophagy Network Restrains Intestinal Stem Cell Proliferation by Counteracting EGFR-ERK Signaling. Developmental cell. 2019;49(4):574–89 e575.
31. Dornhoff H, Becker C, Wirtz S, Strand D, Tenzer S, Rosfa S, et al. A variant of Smurf2 protects mice against colitis-associated colon cancer by inducing transforming growth factor beta signaling. Gastroenterology. 2012;142(5):1183–94 e1184.
32. Kim DG, Lee JY, Lee JH, Cho HY, Kang BS, Jang SY, et al. Oncogenic Mutation of AIMP2/p38 Inhibits Its Tumor-Suppressive Interaction with Smurf2. Cancer research. 2016;76(11):3422–36.
33. Li Y, Yang D, Tian N, Zhang P, Zhu Y, Meng J, et al. The ubiquitination ligase SMURF2 reduces aerobic glycolysis and colorectal cancer cell proliferation by promoting ChREBP ubiquitination and degradation. J Biol Chem. 2019;294(40):14745–56.
34. Zimmer L, Barlesi F, Martinez-Garcia M, Dieras V, Schellens JH, Spano JP, et al. Phase I expansion and pharmacodynamic study of the oral MEK inhibitor RO4987655 (CH4987655) in selected patients with advanced cancer with RAS-RAF mutations. Clinical cancer research: an official journal of the American Association for Cancer Research. 2014;20(16):4251–61.
35. Blumenschein GR Jr, Smit EF, Planchard D, Kim DW, Cadranel J, De Pas T, et al. A randomized phase II study of the MEK1/MEK2 inhibitor trametinib (GSK1120212) compared with docetaxel in KRAS-mutant advanced non-small-cell lung cancer (NSCLC)dagger. Annals of oncology: official journal of the European Society for Medical Oncology. 2015;26(5):894–901.
36. Janne PA, van den Heuvel MM, Barlesi F, Cobo M, Mazieres J, Crino L, et al. Selumetinib Plus Docetaxel Compared With Docetaxel Alone and Progression-Free Survival in Patients With KRAS-Mutant Advanced Non-Small Cell Lung Cancer: The SELECT-1 Randomized Clinical Trial. Jama. 2017;317(18):1844–53.
37. Wee S, Jagani Z, Xiang KX, Loo A, Dorsch M, Yao YM, et al. PI3K pathway activation mediates resistance to MEK inhibitors in KRAS mutant cancers. Cancer research. 2009;69(10):4286–93.

38. Sun C, Hobor S, Bertotti A, Zecchin D, Huang S, Galimi F, et al. Intrinsic resistance to MEK inhibition in KRAS mutant lung and colon cancer through transcriptional induction of ERBB3. Cell reports. 2014;7(1):86–93.
39. Xie J, Xia L, Xiang W, He W, Yin H, Wang F, et al. Metformin selectively inhibits metastatic colorectal cancer with the KRAS mutation by intracellular accumulation through silencing MATE1. Proc Natl Acad Sci USA. 2020;117(23):13012–22.

Figures

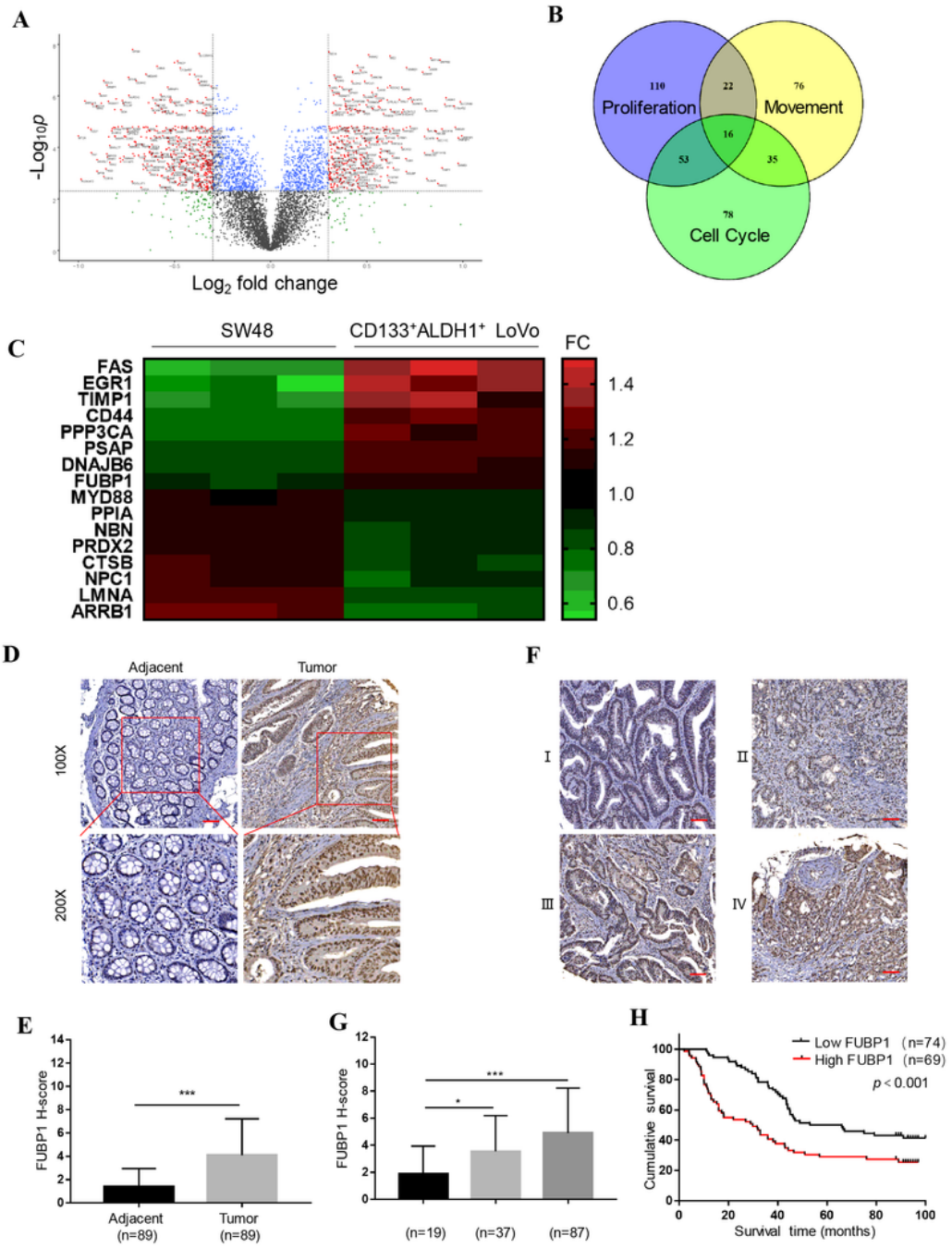

Figure 1

Elevated FUBP1 is associated with tumor progression in CRC. (A) Volcano Plot of differential proteins in CD133+ALDH1+ LoVo cells versus SW48 cells screened by iTRAQ protein mass spectrometry (log2|FC | > 1.2; p < 0.005). (B) Venn diagram of proteins related to cell cycle, proliferation, and movement. (C) Heat map illustrated overlap protein expression. (D) Representative images of FUBP1 IHC staining of 89 adjacent specimens versus 89 CRC specimens in a CRC Tissue Microarray (top, 100× magnification;

bottom, 200× magnification; HCol-Ade180Sur-08-M-088). Scale bar, 50μm. (E) Statistical analysis of FUBP1 staining in adjacent specimens and CRC specimens. IHC quantification was performed using the staining intensity (SI). High FUBP1 expression was considered H-Score ≥ 5; *** p < 0.001. (F) Representative images of FUBP1 IHC staining at different clinical stages (100x magnification). Scale bar, 50μm. (G) Statistical analysis of FUBP1 staining at different clinical stages; * p < 0.05; *** p < 0.001. (H) Overall survival analysis of 89 CRC patients with low versus high FUBP1 expression.

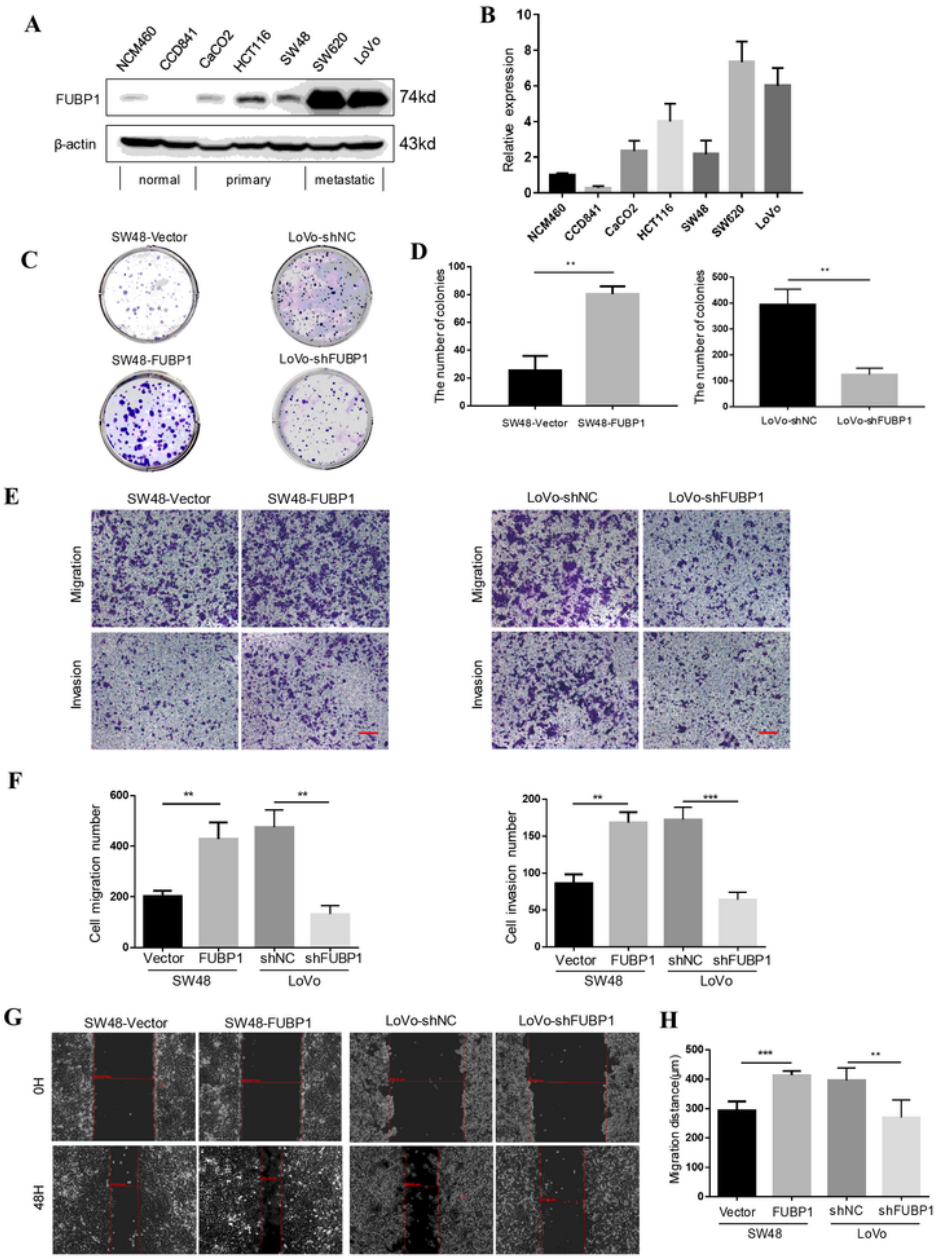

Figure 2

Elevated FUBP1 promotes CRC cell migration and invasion. (A) The protein levels of FUBP1 in CRC cells and normal intestinal epithelial cells by Western blotting analysis. (B) The relative protein expression of FUBP1 was summarized as the mean ±SD of three independent experiments. (C) Representative images of colony formation in the indicated FUBP1-transfected, FUBP1-silenced, or vector control cells. (D) Statistical analysis of colony formation. Bars represent the mean ± SD of three independent experiments; ** $p < 0.01$. (E) Representative images of Transwell assays of migration and invasion by the indicated cells. Scale bar, 100μm. (F) Statistical analysis of cell migration and invasion. Bars represent the mean ± SD of three independent experiments; ** $p < 0.01$; *** $p < 0.001$. (G) Representative images of Wound-healing assays by the indicated cells. (H) Statistical analysis of wound-healing assays. Bars represent the mean ± SD of three independent experiments; ** $p < 0.01$; *** $p < 0.001$.

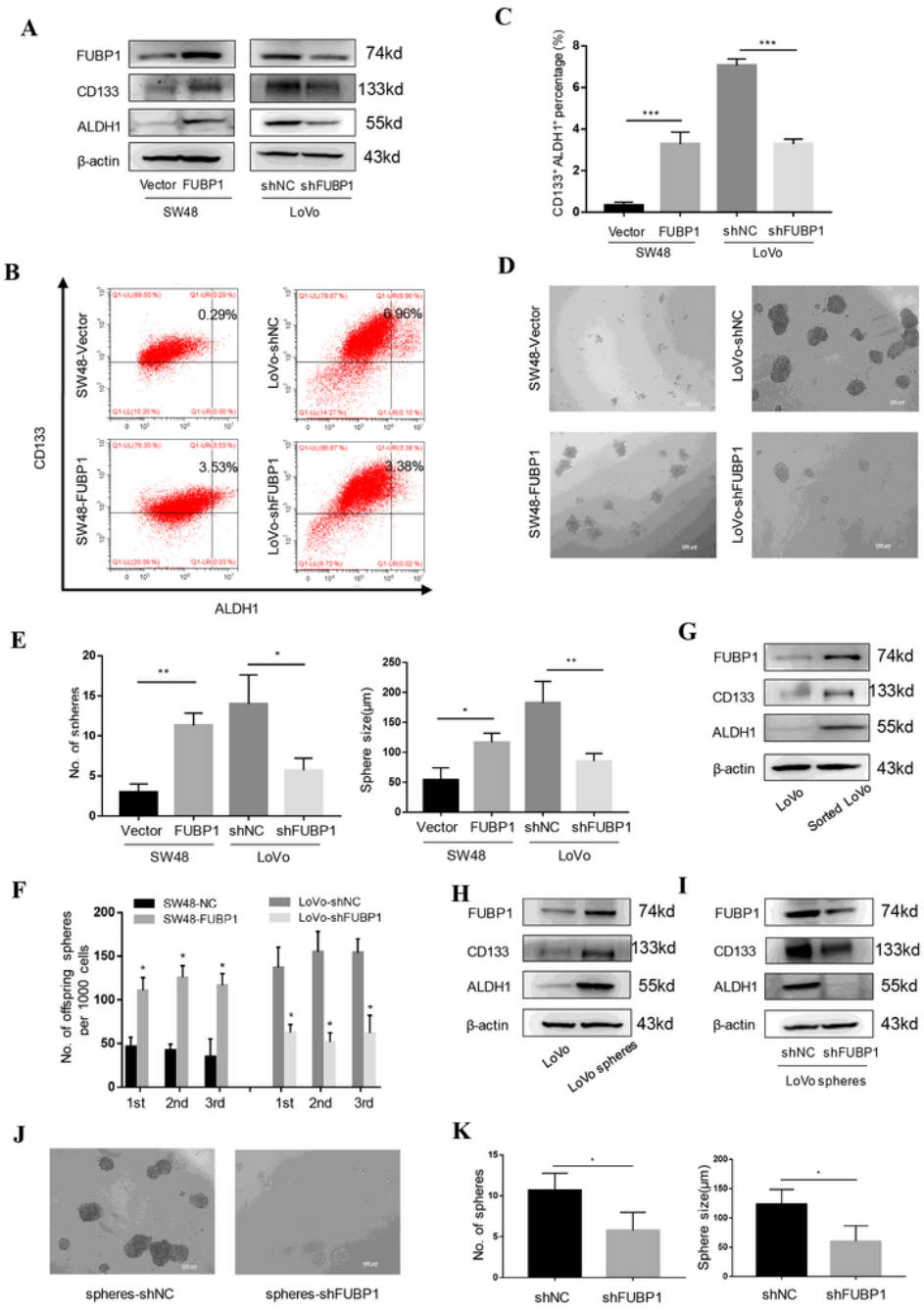

Figure 3

Elevated FUBP1 promotes the stemness of CRC cells in vitro. (A) Western blotting analysis of stemness-related markers, CD133 and ALDH1, in the indicated cells. β-Actin served as a loading control. (B) Flow cytometric analysis proportion of the co-expression of CD133-PE and ALDH1-FITC in the indicated cells. (C) Statistical analysis of the proportion of CD133+ALDH1+ cells. Bars represent the mean ± SD of three independent experiments; *** $p < 0.001$. (D) Representative images of tumor sphere formation after ten

days in nonadherent cultures of the indicated cells. Scale bar, 100μm. (E) Statistical analysis of sphere numbers and sizes after ten days in nonadherent cultures of the indicated cells. Bars represent the mean ± SD of three independent experiments; * $p < 0.05$; ** $p < 0.01$. (F) The number of serially passaged spheroids was summarized as the mean ± SD of three independent experiments; * $p < 0.05$. (G) Western blotting analysis of FUBP1 in LoVo cells and CD133+ALDH1+ cells sorted from LoVo cells. (H) Western blotting analysis of FUBP1 in LoVo cells and LoVo spheres. (I) Western blotting analysis of CD133 and ALDH1 in FUBP1-silenced cells and vector control cells, which were CD133+ALDH1+ cells sorted from LoVo cells. (J, K) Representative micrographs (J) and quantification (K) of tumor sphere formation by FUBP1-silenced LoVo spheres and its control LoVo spheres. Bars represent the mean ± SD of three independent experiments; * $p < 0.05$. Scale bar, 100μm.

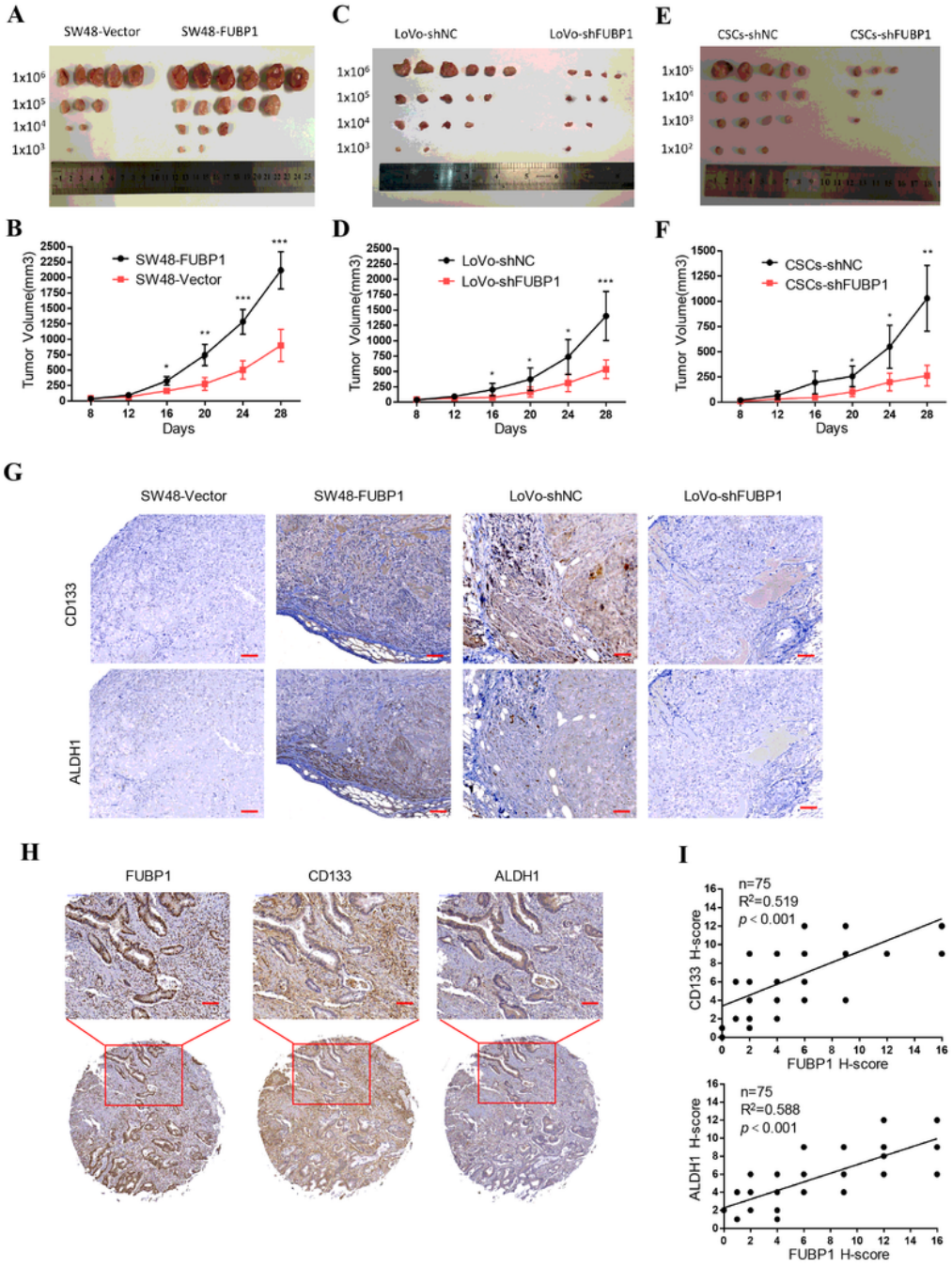

Figure 4

Elevated FUBP1 enhances the tumorigenicity of CRC cells in vivo. (A, C, E) Representative images of the tumors were shown. (A) Tumors formed by FUBP1-transfected SW48 cells and vector control. (C) Tumors formed by FUBP1-silenced LoVo cells and control LoVo cells. (E) Tumors formed by FUBP1-silenced cells which were CD133+ALDH1+ cells sorted from LoVo cells and its control cells. Cells (1×106, 1×105, 1×104, 1×103 or 1×102) were implanted into BALB/c nude mice (n=6, per group). Tumor formation growth

curves following implantation of the 1×106 (B) (D)or 1×105 (F) indicated cells. (G) Representative images of IHC staining of CD133, ALDH1, and FUBP1 in tumor tissues of mice originated from the indicated cells. Scale bar, 50μm. (H) Representative images of FUBP1, CD133, and ALDH1 IHC staining of CRC Tissue Microarrays (HCol-A150CS-02-M-013, 75 cases). Scale bar, 100μm. (I) Correlation analysis of FUBP1 expression with the expression of CD133 and ALDH1 in 75 CRC patient specimens. All data are presented as mean±S.D., and *, **and*** denotes $p < 0.05$, $p < 0.01$, and $p < 0.001$, respectively.

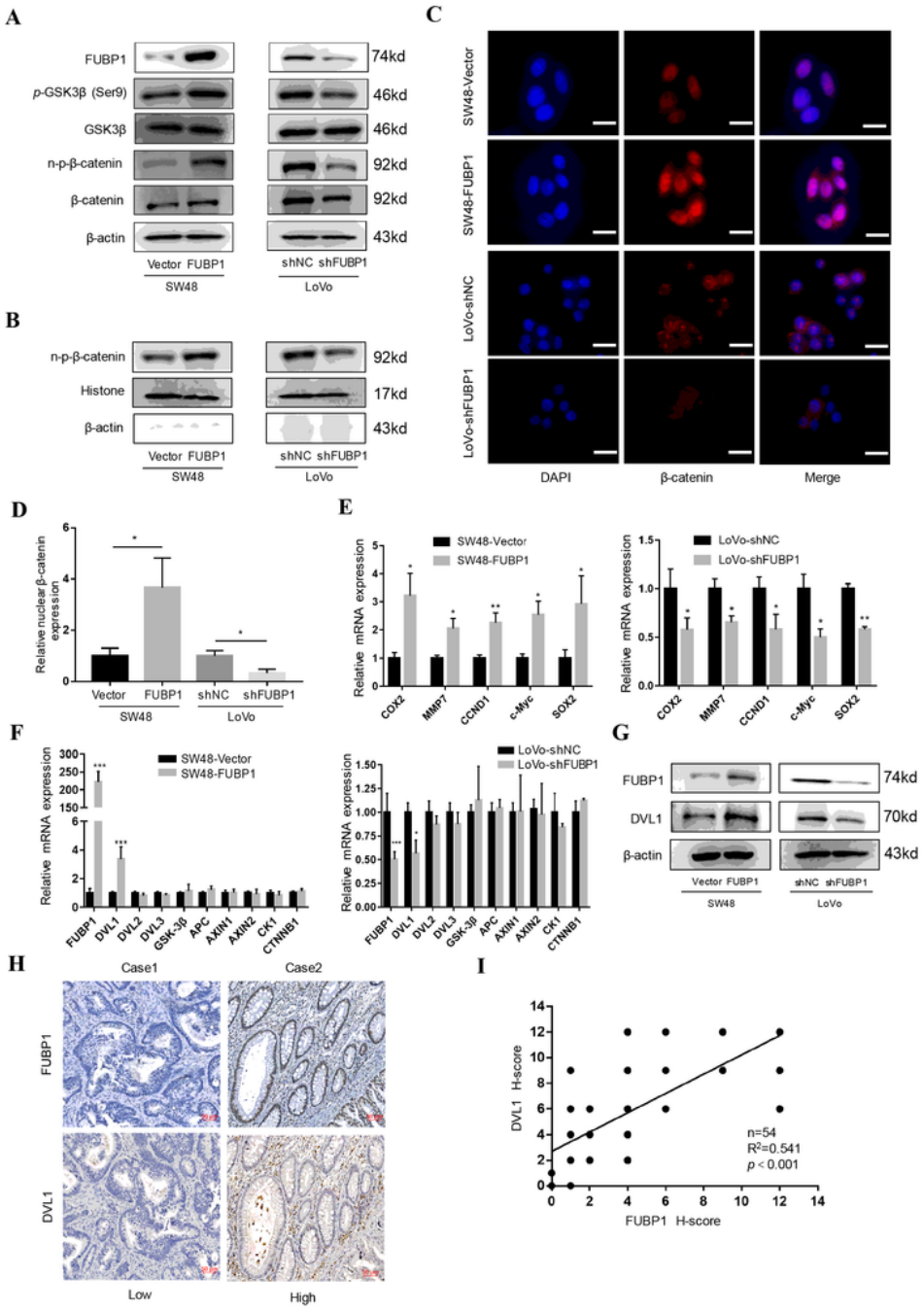

Figure 5

Elevated FUBP1 activates the Wnt/β-catenin signaling. (A) Western blotting analysis of Wnt/β-catenin signaling in the indicated FUBP1-transfected, FUBP1-silenced, and vector control cells. (B) Western blotting analysis of β-catenin in the nuclear fractions of the indicated cells. (C, D) Immunofluorescence staining(C) and quantification(D) of nuclear β-catenin expression in the indicated cells; * $p < 0.05$. (E) The mRNA levels of β-catenin downstream genes by Real-time PCR in the indicated cells. Bars represent the mean ± SD of three independent experiments; * $p < 0.05$; ** $p < 0.01$. (F) The mRNA levels of key scaffold molecules in the upstream of β-catenin genes by Real-time PCR in the indicated cells. Bars represent the mean ± SD of three independent experiments; * $p < 0.05$; ** $p < 0.01$; *** $p < 0.001$. (G) Western blotting analysis of DVL1 in the indicated cells. (H) Immunohistochemistry staining of DVL1 in 54 CRC specimens which collected from Sun Yat-sen University Cancer Center. Two representative cases are shown. Scale bar, 50μm. (I) Correlation analysis of DVL1 expression with FUBP1 expression in CRC specimens; *** $p < 0.001$.

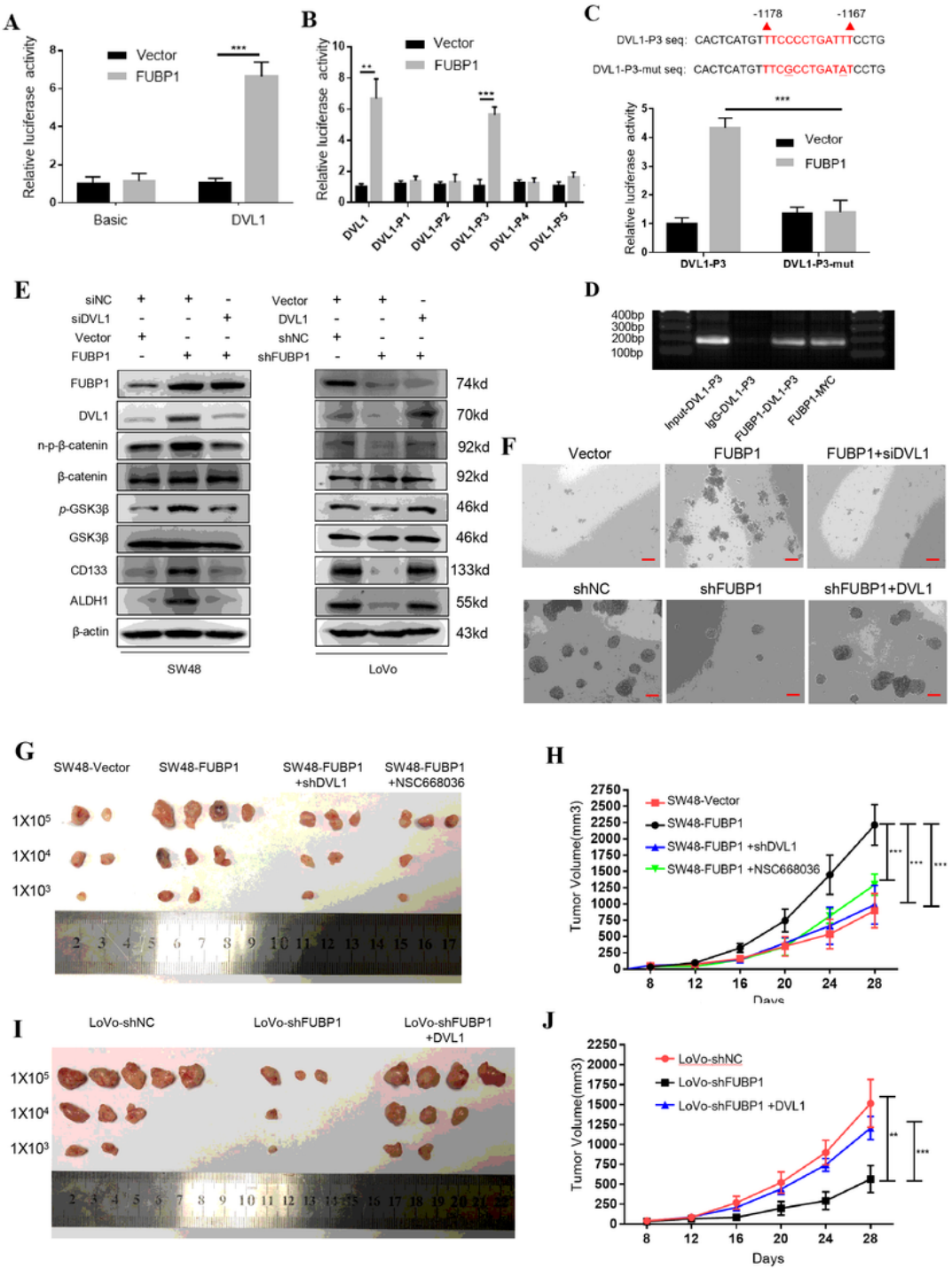

Figure 6

FUBP1 up-regulates DVL1 through direct binding to its promoter. (A) Luciferase reporter assays of DVL1 promoter transcriptional activity. LoVo cells were infected with FUBP1-overexpressing plasmid or empty vector plasmid, DVL1 promoter-luciferase reporter plasmid, and Renilla luciferase plasmid for 48 h, followed by fluorescence detection. Renilla luciferase served as the transfection control. Bars represent the mean ± SD of three independent experiments; *** $p < 0.001$. (B) Luciferase reporter assays of DVL1

promoter truncation fragments included P1, P2, P3, P4, and P5 transcriptional activity. Bars represent the mean ± SD of three independent experiments; ** $p < 0.01$; *** $p < 0.001$. (C) Luciferase reporter assays of mutant DVL1-P3 promoter transcriptional activity. LoVo cells were infected with FUBP1-overexpressing plasmid or empty vector plasmid, wild-type DVL1-P3 promoter-reporter, and mutant reporter (C to G substitution and T to A substitution, underlined) for 48 h, followed by fluorescence detection. Bars represent the mean ± SD of three independent experiments; *** $p < 0.001$. (D) Chip assays were performed to verify FUBP1 binding to the DVL1-P3 promoter. Lane 1: PCR product from input DNA; Lane 2: PCR product from immunoprecipitated by normal IgG; Lane 3: PCR product derived from immunoprecipitation by an anti-FUBP1 antibody; Lane 4: PCR product derived from immunoprecipitation by anti-c-Myc antibody. (E, F) Effects of FUBP1 on Wnt/β-catenin signaling (E) and tumor sphere formation (F) were blocked after knockdown of DVL1 or recover after overexpression of DVL1. Scale bar, 100μm. (G, H) The representative morphology (G) and tumor growth rate (H) were shown in SW48-Vector, SW48-FUBP1, SW48-FUBP1+shDVL1, and SW48-FUBP1+ NSC668036 xenograft models. (I, J) The representative morphology (I) and tumor growth rate (J) were shown in LoVo-shNC, LoVo-shFUBP1, and LoVo-shFUBP1 + DVL1 xenograft models.

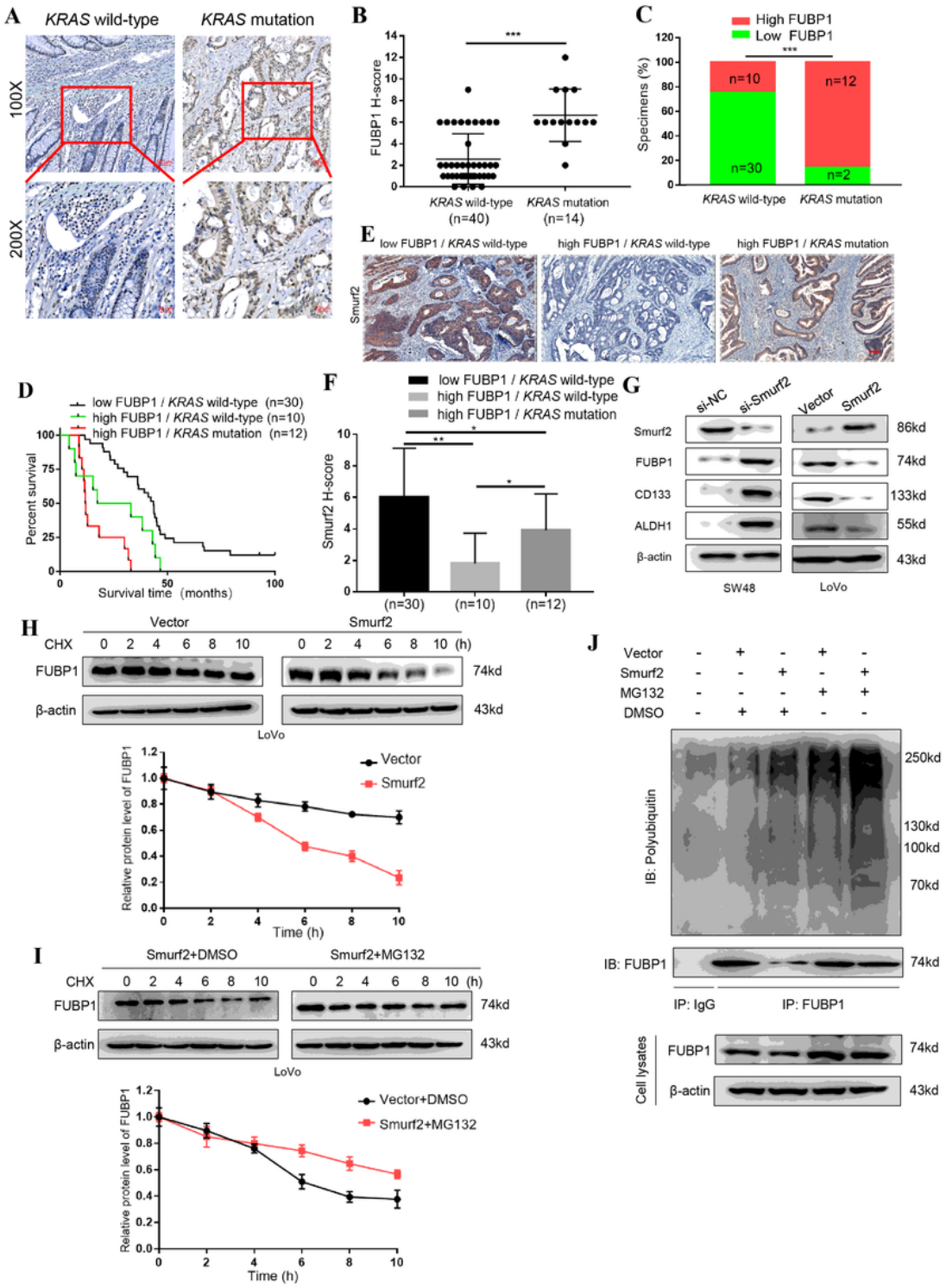

Figure 7

FUBP1 is ubiquitinated by Smurf2 in CRC regardless of KRAS genotype. (A) Representative images of FUBP1 IHC staining of 40 KRAS wild-type CRC specimens versus 14 KRAS mutation CRC specimens collected from Sun Yat-sen University Cancer Center (top, 100× magnification; bottom, 200× magnification). Scale bar, 50μm. (B, C) Statistical analysis of the 54 CRC specimens showing low or high FUBP1 expression relative to KRAS wild-type or KRAS mutation. *** $p < 0.001$. (D) Overall survival

analysis of 52 CRC patients which divided into three groups: KRAS wild-type and low FUBP1 expression (n = 30); KRAS wild-type and high FUBP1 expression (n = 10); KRAS mutation and high FUBP1 expression (n = 12); * $p < 0.05$; *** $p < 0.001$. (E) Representative images of Smurf2 IHC staining in three groups according to FUBP1 expression (high or low) and KRAS mutation or wild-type. Scale bar, 100μm. (F) Statistical analysis of Smurf2 staining in three groups; * $p < 0.05$; ** $p < 0.01$. (G) Western blotting analysis of FUBP1, CD133 and, ALDH1 in the indicated cells. β-Actin served as a loading control. (H, I) Cycloheximide chase assay of FUBP1. (H) LoVo cells transiently transfected with vector or Smurf2 plasmids were treated with cycloheximide (CHX, 10μg/ml) for indicated time points and then collected for western blotting analysis. (I) LoVo cells transfected with Smurf2 plasmid were treated with DMSO or MG132 (10μmol/l) in the presence of CHX (10μg/ml) for indicated time points and then collected for western blotting analysis. (J) LoVo cells transiently transfected with Vector or Smurf2 plasmids were treated with DMSO or MG132 (10μmol/L) for 12h, and then immunoprecipitated with an FUBP1 antibody.

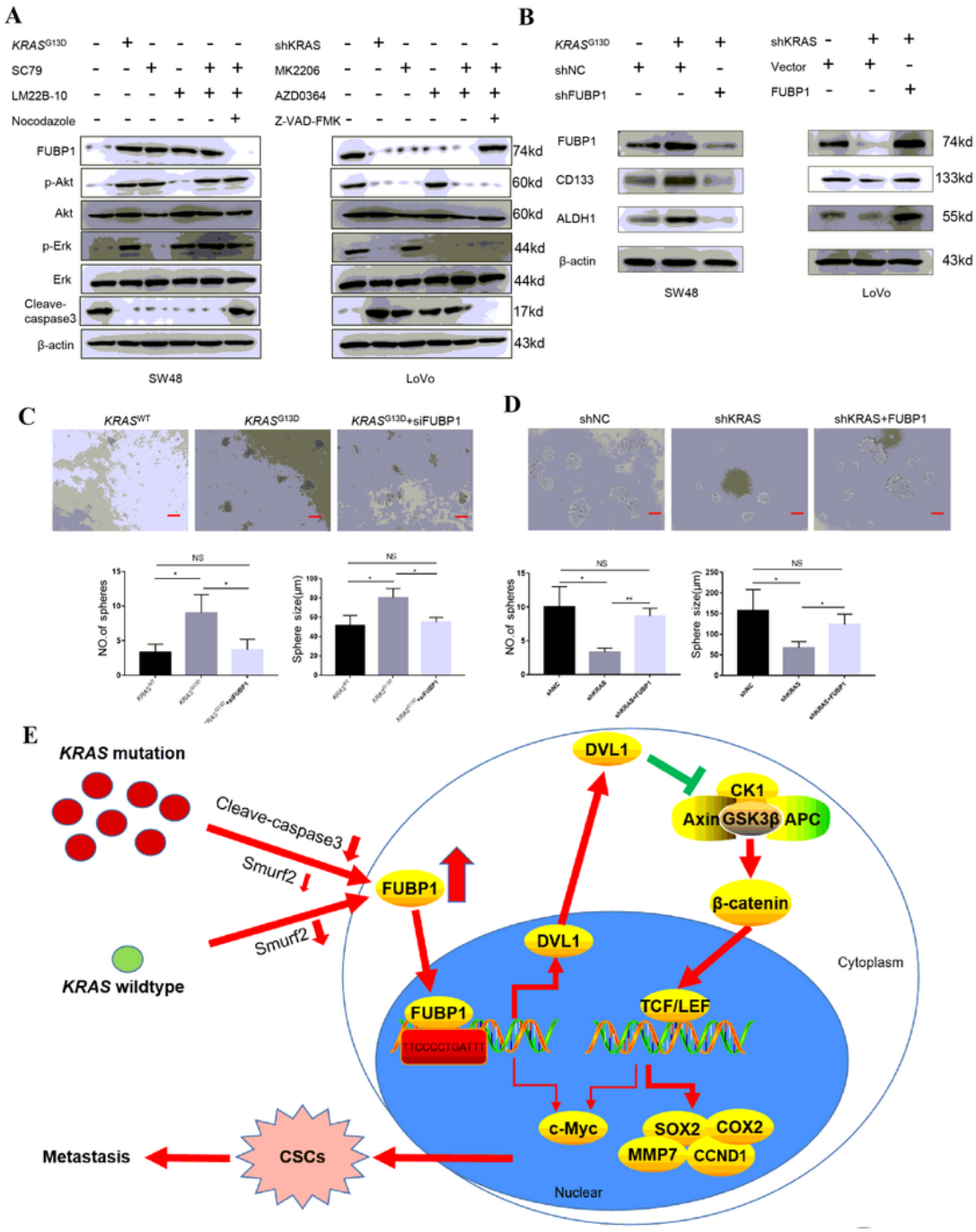

Figure 8

FUBP1 is also up-regulated by caspase3 inactivation driven by KRAS signaling in KRAS mutation CRC. (A)Western blotting analysis of FUBP1, phosphorylated AKT, total AKT, phosphorylated ERK, total ERK and Cleave-caspase3 in SW48 cells with KRAS mutation or AKT, ERK, apoptosis activators and in LoVo cells with KRAS-silencing or AKT, ERK, apoptosis inhibitors. (B, C, D) Effects of KRAS mutation on stem-related markers (B) and tumor sphere formation (C, D) were blocked after knockdown of FUBP1 or recover

after overexpression of FUBP1. Bars represent the mean ± SD of three independent experiments; * $p < 0.05$; ** $p < 0.01$. Scale bar, 100μm. (E)The schematic overview of the potential mechanism involved in FUBP1 overexpression promotes the stemness of CRC cells.

Supplementary Files

This is a list of supplementary files associated with this preprint. Click to download.

- supplymentFigure1.tif
- supplymentFigure2.tif
- supplymentFigure3.tif
- supplymentFigure4.tif
- supplymentFigure5.tif
- supplymentFigure6.tif
- supplymentFigure7.tif
- supplymentFigure8.tif
- supplymentFigure9.tif
- supplymentFigure10.tif
- supplymentFigure11.tif
- supplymentFigure12.tif
- supplymentFigure13.tif